

Electron Diffraction Investigation of Dimethyl Diselenide

P. D'ANTONIO, C. GEORGE, A. H. LOWREY, AND J. KARLE

Naval Research Laboratory, Washington, D. C. 20390

(Received 11 February 1971)

The molecular structure of dimethyl diselenide has been determined by an electron diffraction investigation of the vapor. A computerized background correction routine, satisfying the positivity and area criteria, was employed to reduce the data and obtain a final molecular intensity curve. The values for a set of nine distances and amplitudes were obtained from a least-squares fit to the final molecular intensity curve. The bonded distances are $r_p(\text{C-H}) = 1.131 \pm 0.008$ Å, $r_p(\text{C-Se}) = 1.954 \pm 0.005$ Å, and $r_p(\text{Se-Se}) = 2.326 \pm 0.004$ Å. The corresponding amplitudes are $l(\text{C-H}) = 0.079 \pm 0.007$ Å, $l(\text{C-Se}) = 0.054 \pm 0.003$ Å, and $l(\text{Se-Se}) = 0.056 \pm 0.002$ Å. The $\angle \text{CSeSe} = 98.9 \pm 0.02^\circ$ and the $\angle \text{HCSe} = 108.4 \pm 0.8^\circ$. The errors are estimated to be at the 99% confidence level. The methyl groups are unsymmetrically placed with respect to the CSeSe planes. They are rotated about the C-Se bonds such that one of the HCSe planes in each CH_3Se moiety makes an angle of $36.1 \pm 6^\circ$ with the respective CSeSe plane. Dimethyl diselenide assumes a stable skew conformation with a dihedral angle of $87.5 \pm 4^\circ$. The molecule contains a twofold axis of symmetry passing midway between the two selenium atoms in the plane bisecting the dihedral angle.

INTRODUCTION

Recently, the vibrational spectra and structure of $(\text{CH}_3\text{-Se})_2$ were investigated by Green and Harvey.¹ The molecule was found to possess C_2 symmetry with an estimated dihedral angle of $\sim 82^\circ$ obtained from a best fit to the observed vapor-phase band contours. The fundamental vibrations, with the exception of the methyl torsion, have been assigned and supported by a normal coordinate analysis. Since no structural data were available for $(\text{CH}_3\text{-Se})_2$, Green and Harvey used an assumed model in their normal coordinate analysis.

The only vapor-phase structural data reported in the literature for substituted diselenides concern $(\text{CF}_3\text{-Se})_2$, which was investigated by Bowen² in 1954. Using the visual method he obtained the three bonded distances from electron diffraction data. All bond angles were assumed. There are several investigations on substituted diselenides in the solid state which can be examined in a forthcoming review by Karle.³

The investigation of the detailed molecular structure of $(\text{CH}_3\text{-Se})_2$ was undertaken with the intent to facilitate a more accurate force model investigation and to make a start at filling in the void of structural information which exists for substituted diselenides in the vapor phase.

DATA REDUCTION AND STRUCTURE DETERMINATION

Dimethyl diselenide is a deeply colored, reddish-orange liquid, which boils at 153°C (760 mm) and has an extremely offensive odor. The sample was prepared by Green and Harvey and no significant impurities were detected by NMR and mass spectrometry.

A pulsed burst nozzle, with a 0.15-mm orifice, was employed in the diffraction apparatus⁴ and the temperature of the vapor in the nozzle reservoir was $100 \pm 5^\circ\text{C}$. The photographs were multiple exposures of 0.2–0.4-sec duration using s , s^2 , and s^3 sectors at a fixed camera distance of ~ 11 cm. The specimen-to-plate

distance was measured independently for each plate and the voltage (~ 40 kV) was continuously monitored with a digital voltmeter at the low voltage tap of a precision (0.0025%) resistance bank. Photographs of CS_2 were taken as a check on the scale of the molecule. Kodak contrast photographic emulsion plates were used and developed in nitrogen-agitated Kodak Dektol solution. The rotating⁵ photographic plates were scanned with a modified Leeds and Northrup microdensitometer equipped to punch four-digit transmittance and position data onto paper tape. The transmittance data were converted to intensity⁶ at intervals of 0.1 s unit. The total intensities from the left and right sides of each scan were averaged. These average total intensities were processed with an automated background correction routine based on the positivity and area criteria. The function used in the calculation of a background line was

$$b_p(s) = \exp(\alpha_p + \beta_p s^{\gamma_p}). \quad (1)$$

The actual background line $B_n(s)$ is generated from a weighted average of segments $b_p(s)$, each having independent values for the background constants, α_p , β_p , and γ_p ,

$$B_p(s) = [u_p(s)B_{p-1}(s) + v_p(s)b_p(s)], \quad p = 1, \dots, n, \quad (2)$$

where p represents the number of the segment in a set of n segments and $u_p(s)$ and $v_p(s)$ are weighting coefficients in the overlap range of two segments. $B_0(s) = 0$ and $B_1(s) = b_1(s)$, the first segment. The weighting coefficients assume the form shown in Fig. 1.

The values for the background constants α_p , β_p , and γ_p were determined in two ways:

(1) The experimental total intensity function at the null points of a theoretical model is divided into three-point segments (1, 2, 3; 2, 3, 4; etc., or 1, 3, 5; 2, 4, 6; etc., where the digits label the successive null points).

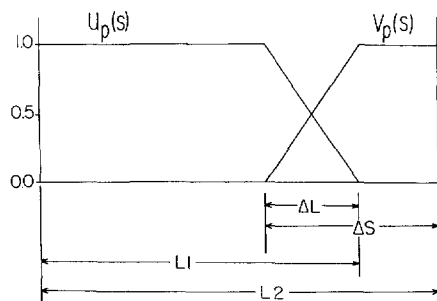


FIG. 1. Diagram representing a stage in the application of Eq. (2). L_1 is the range of $B_{p-1}(s)$; L_2 is the range of $B_p(s)$; Δs is the range of $b_p(s)$; ΔL is the range of overlap of $B_{p-1}(s)$ and $b_p(s)$.

The background constants are then determined for each segment by a three-point fit.

(2) The background function, $I_b(s)$, is generated from the experimental total intensity function, $I_m(s)$, using the following relation⁷:

$$I_b(s) = I_t(s) / [I_m(s) + 1]. \quad (3)$$

$I_m(s)$ may be obtained from either of two types of calculation which will be described in detail below. It can be either a trial theoretical molecular intensity function or the corrected Fourier sine transform of a positimized radial distribution curve, $f(r)$. $I_b(s)$ is segmented into intervals, Δs , ranging from 8 to 1 s unit. Each segment may be displaced from the preceding one by an arbitrary amount. The background constants are determined from a least squares fit to each segment using Eq. (1).

The initial molecular intensity functions were obtained from Eq. (4),⁷

$$I_m(s) = [I_t(s) / B_n(s)] - 1, \quad (4)$$

using the background functions, $B_n(s) \sim I_b(s)$, developed in step (1) by means of the three-point fits. The resulting molecular intensities were averaged and a theoretical molecular intensity function was attached in the inner region, $0 \leq s \leq 2.8$. This molecular intensity curve was corrected for nonconstant scattering factors⁸ prior to being transformed into the corresponding radial distribution curve, $f(r)$. The correction term $\Delta I_m(s)$ was calculated from the following equations. The theoretical expression for the molecular intensity $sI_m(s)$ is given by

$$sI_m(s) = K \sum_{i \neq j}^N \sum_1 \sigma_{ij}(s) \cos \Delta \eta_{ij}(s) \times \exp(-\frac{1}{2} \langle l_{ij}^2 \rangle s^2) \sin(sr_{ij}) / r_{ij}, \quad (5)$$

where

$$\sigma_{ij}(s) = f_i(s) f_j(s) / \sum_{k=1}^N \left[\frac{f_k^2(s) + S_k(s)}{s^4} \right].$$

K is a scale factor, N is the total number of atoms, $\langle l_{ij}^2 \rangle$ is the mean-squared amplitude of vibration

between the i th and j th atoms having an internuclear distance r_{ij} , s is a function of scattering angle and electron wavelength equal to $[4\pi \sin(\frac{1}{2}\theta)] / \lambda$, $f_i(s)$ and $\eta_i(s)$ are the magnitude and phase, respectively, of the partial wave elastic scattering factor for the i th atom, tabulated by Cox and Bonham,⁹ and $S_i(s)$ is the inelastic scattering factor tabulated by Tavard *et al.*¹⁰

The functional counterpart of $sI_m(s)$ with constant coefficients, $sI_c(s)$, is given by

$$sI_c(s) = K \sum_{i \neq j}^N \sum_1 \bar{g}_{ij} \cos \Delta \eta_{ij}(s) \times \exp(-\frac{1}{2} \langle l_{ij}^2 \rangle s^2) \sin(sr_{ij}) / r_{ij}, \quad (6)$$

where

$$\bar{g}_{ij} = \langle \sigma_{ij}(s) \rangle_s,$$

and s_r represents s values restricted to the experimental range.

The nonconstant coefficient correction is⁸

$$\Delta s I_m(s) = s I_m(s) - s I_c(s), \quad (7)$$

and the constant coefficient radial distribution curve is computed from

$$f(r) = \left(\frac{2}{\pi} \right)^{1/2} \int_0^{s_{\max}} [s I_m(s) - \Delta s I_m(s)] \times \exp(-as^2) \sin(sr) ds. \quad (8)$$

In this experiment the damping factor a was set so that $as_{\max}^2 = 3$.

The resulting radial distribution curve was set to zero in all regions where the probability of finding an internuclear distance is zero. This was accomplished by fitting the lower 50% of the physically significant peaks in the radial distribution curve with Gaussian functions and averaging these Gaussian extensions with the existing peaks to provide a continuous fall to zero. An improved molecular intensity function was obtained from the Fourier sine transform of the positimized radial distribution curve. It was adjusted to the variable coefficient form for use in Eq. (3) by adding the correction term $\Delta s I_m(s)$ given by Eq. (7). A new set of background curves, $I_b(s)$, were generated with the improved molecular intensity function using Eq. (3). These background lines were fit as described in step (2) above and a corresponding new set of molecular intensity curves was obtained from Eq. (4). The intensity curves were averaged, an inner region from the improved molecular intensity function was added, and the combined curve was transformed. A preliminary least squares fit was made to both the combined molecular intensity curve and the constant coefficient radial distribution curve $f(r)$. From these procedures a further improved molecular intensity function was obtained. The positivity adjustment of the radial distribution function and the least squares procedures were repeated while decreasing the fitting range, Δs , until a positive radial distribution curve was obtained from smooth background lines,

$B_n(s)$, for each of the photographic plates used in the analysis. After each cycle $I_m(s)$, $I_b(s)$, $I_t(s)$, and $B_n(s)$ were displayed for inspection. The last three curves were leveled by multiplying each by Eq. (1) in which the values for α , β , and γ were determined from a fit to three widely spaced points on the $B_n(s)$ curve. As the data reduction procedure progressed, the generated background lines, $I_b(s)$, Eq. (3), more closely resembled their smooth counterparts, $B_n(s)$, Eq. (2). In the final cycle the generated background lines were featureless curves.

RESULTS AND DISCUSSION

The final values for a set of nine equilibrium distances and nine root-mean-squared amplitudes of vibration were obtained from a least squares fit to the final

TABLE I. r_o distances, angles, and thermal parameters in dimethyl diselenide. Errors are estimated at the 99% confidence level.

	$r_o(\text{\AA})$	$(I_i^2)^{1/2}(\text{\AA})$
C-H	1.131 ± 0.008	0.079 ± 0.007
C-Se	1.954 ± 0.005	0.054 ± 0.003
Se-Se	2.326 ± 0.004	0.056 ± 0.002
Se...H _S	2.552 ± 0.011	0.153 ± 0.010
Se...H _{L1}	3.095 ± 0.023	0.082 ± 0.030
C...Se	3.263 ± 0.008	0.099 ± 0.005
Se...H _{L2}	3.610 ± 0.027	0.085 ± 0.034
C...C	3.966 ± 0.038	0.105 ± 0.037
Se...H _{L3}	4.248 ± 0.036	0.105 ± 0.037
$\angle \text{CSeSe}$	$98.9^\circ \pm 0.2^\circ$	
$\angle \text{HCSe}$	$108.4^\circ \pm 0.8^\circ$	
$\phi(\text{HCSeSe})$	$36.1^\circ \pm 6^\circ$	
$\tau(\text{CSeSeC})$	$87.5^\circ \pm 4^\circ$	

molecular intensity curve using Eq. (5) which contains variable coefficients. In carrying out the least squares analysis, it was assumed that the molecule had C_2 symmetry and that the methyl groups had C_3 symmetry about the C-Se bond. The least squares parameters are listed in Table I, and the atomic coordinates are listed in Table II. The final errors quoted are at the 99% confidence level. The three bonded distances and the CSeSe and the HCSe angles are shown together with the spatial geometry, looking down the twofold axis in Fig. 2.

A theoretical molecular intensity curve was calculated, using Eq. (5), from the values in Table I and the remaining C...H and H...H nonbonded distances and amplitudes. The rms amplitudes for the nonbonded C...H and H...H distances were assumed to be 0.15 Å. In Fig. 3 the theoretical molecular intensity curve is shown together with the experimental curve and their difference. The experimental molecular intensity data have been deposited with ASIS-NAPS.¹¹ The corre-

TABLE II. Atomic coordinates associated with r_o distances.

Atom	x	y	z
C(1)	-0.3019	-1.9299	0.0000
Se(1)	0.0000	0.0000	0.0000
C(2)	2.6273	-0.0842	1.9280
Se(2)	2.3254	0.0000	0.0000
H(11)	0.4961	-2.4138	0.6291
H(12)	-1.3214	-2.1294	0.4330
H(13)	-0.2449	-2.2979	-1.0621
H(21)	1.8293	-0.7337	2.3841
H(22)	3.6468	-0.5255	2.1085
H(23)	2.5703	0.9609	2.3420

sponding experimental and theoretical radial distribution curves and their difference are shown in Fig. 4. A decomposition of the experimental radial distribution curve into nine Gaussian peaks, representing the set of nine distances listed in Table I, is illustrated in Fig. 5. The experimental radial distribution curve was multiplied by r to enhance the features in the outer region of the curve thus enabling the longer distances to be depicted.

The bonded C-Se, Se-Se, and the nonbonded C...Se distances occur at 1.954, 2.326, and 3.263 Å, respectively. The six short Se...H_S distances, in the CH₃Se moieties, appeared as a shoulder on the Se-Se peak at 2.552 Å. The remaining structural features are the methyl torsional angle ϕ (HCSeSe) and the dihedral angle τ (CSeSeC).

The magnitude of ϕ is dependent upon the three long Se...H distances (Se...H_{L1}, Se...H_{L2}, Se...H_{L3}), located at 3.095, 3.610, and 4.248 Å, respectively. Each long Se...H distance yields a value for ϕ , and a final

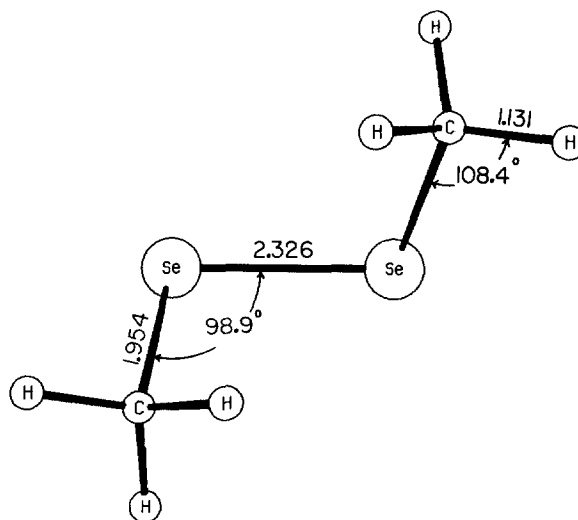


FIG. 2. Spatial geometry and molecular parameters of dimethyl diselenide.

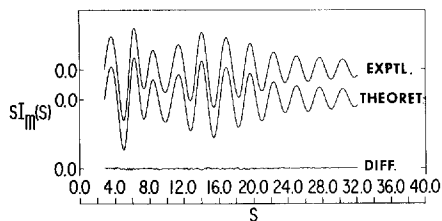


FIG. 3. Experimental molecular intensity, theoretical molecular intensity, and their difference for dimethyl diselenide.

value of 36.1° is an average of the three results. Angle $\phi=0^\circ$ when the hydrogen in the HCSeSe group is *cis* to the farthest selenium atom and a positive rotation is defined as a counterclockwise rotation looking down the C-Se bond. Although the data do not afford a clear-cut determination of the sense of the rotation, the generated background line, $I_b(s)$, determined from $\phi=+36.1^\circ$ on the low angle data in the region approximately $3 \leq s \leq 10$, was smoother than $I_b(s)$ derived from $\phi=-36.1^\circ$ and hence, $\phi=+36.1^\circ$ was selected. The fact that the area analysis clearly indicated three distinct long $\text{Se} \cdots \text{H}$ distances, rather than two, suggested that the CH_3 groups are not symmetrically placed with respect to the CSeSe planes ($\phi=0$). That is, the methyl groups seem to be rotated about the C-Se bonds such that one of the HCSe planes in each CH_3Se moiety does not lie in the respective CSeSe plane, but is rotated with respect to this plane by 36.1° . The torsional angle, ϕ , is illustrated in Fig. 6(a) in a view down one of the C-Se bonds.

The dihedral angle is a very significant structural parameter in molecules containing substituted Group VI atoms bonded together (R_2X_2 where R is H, CH_3 , C_6H_5 , etc., and X is O, S, Se, Te). These molecules exist in stable skew configurations with a dihedral angle between ~ 70 – 120° [see Fig. 6(b)]. The dihedral angle in $(\text{CH}_3\text{-Se})_2$ was found to be 87.5° . It is dependent upon the skeletal parameters and the $\text{C} \cdots \text{C}$ distance at 3.966 \AA . Since the scattering from the heavier selenium atoms predominates and partially obscures the contribution from the lighter atoms, the larger limits of error associated with the dihedral angle and the methyl

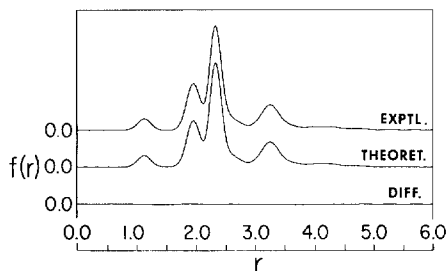


FIG. 4. Experimental radial distribution, theoretical radial distribution, and their difference for dimethyl diselenide.

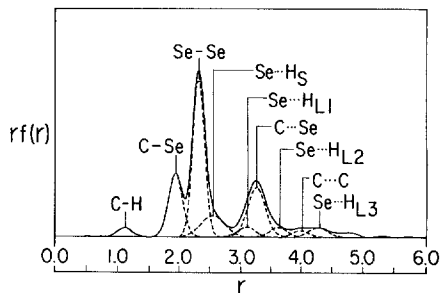


FIG. 5. Partially decomposed experimental radial distribution curve, $rf(r)$, dimethyl diselenide.

torsional angle reflect this characteristic of the scattering.

The molecule possesses a twofold axis of symmetry which lies midway between the two selenium atoms in the plane bisecting the dihedral angle. The twofold symmetry is apparent in Fig. 6(b), which is a view of the molecule down the Se-Se bond. The orientation of the methyl groups is illustrated in Fig. 6(c) in a view down the line connecting the carbon atoms. The three hydrogen atoms on the methyl group which lies below the plane of the paper are indicated by dashed circles.

The bonded Se-Se distance of 2.326 \AA agrees favorably with the value 2.33 \AA obtained in perfluorodimethyl diselenide,² selenium diselenocyanate,¹² *p,p'*-dichlorodiphenyl diselenide,¹³ and the value 2.32 \AA found in 1,2-diselenane-3,6-dicarboxylic acid.¹⁴ It is slightly larger than the values 2.29 and 2.285 \AA found in diphenyl diselenide¹⁵ and bisdiphenylmethyl diselenide,¹⁶ respectively. Except for perfluorodimethyl diselenide these structures have been investigated in the crystalline state.

The C-Se distance of 1.954 is slightly larger than 1.93 \AA obtained in perfluorodimethyl diselenide,² but falls within the range (1.95 – 1.99 \AA) of aliphatic C-Se distances observed in the crystalline state.³

The dihedral angle obtained in this study, 87.5° , is

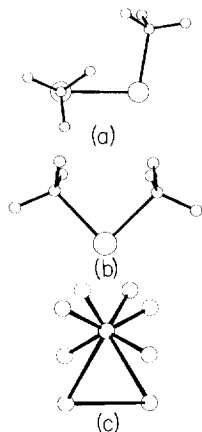


FIG. 6. (a) View of $(\text{CH}_3)_2\text{Se}_2$ down one of the C-Se bonds; (b) view of the molecule down the Se-Se bond; (c) view of the molecule down the line connecting the two carbon atoms.

larger than the value 85° determined for dimethyl disulfide¹⁷ by microwave spectroscopy and the value 82° found in diphenyl diselenide¹⁵ and bisdiphenylmethyl diselenide.¹⁶

ACKNOWLEDGMENTS

The authors wish to express their thanks to Dr. W. H. Green and Dr. A. B. Harvey for suggesting this investigation and providing the $(\text{CH}_3\text{-Se})_2$ sample. We also wish to thank Mr. S. Brenner for his advice in preparing the computing programs.

¹ W. H. Green and A. B. Harvey, *J. Chem. Phys.* **49**, 3586 (1968).

² H. J. M. Bowen, *Trans. Faraday Soc.* **50**, 452 (1954).

³ I. L. Karle and J. Karle, "X-Ray Diffraction," in *Organic Selenium and Tellurium Compounds*, edited by W. H. H. Gunther and D. L. Klayman (Wiley, New York, to be published).

⁴ J. Karle, "Electron Diffraction," in *Determination of Organic Structures by Physical Methods*, edited by F. C. Nachod and J. J. Zuckerman (Academic, New York, to be published).

⁵ I. L. Karle, D. Hooper, and J. Karle, *J. Chem. Phys.* **15**, 765 (1947).

⁶ J. Karle and I. L. Karle, *J. Chem. Phys.* **18**, 957 (1950).

⁷ I. L. Karle and J. Karle, *J. Chem. Phys.* **17**, 1052 (1949).

⁸ L. S. Bartell, L. O. Brockway, and R. H. Schwendeman, *J. Chem. Phys.* **23**, 1854 (1955).

⁹ H. L. Cox, Jr. and R. A. Bonham, *J. Chem. Phys.* **47**, 2599 (1967).

¹⁰ C. Travad, D. Nicolas, and M. Rouault, *J. Chim. Phys.* **64**, 540 (1967).

¹¹ A listing of s vs $sI_m(s)$ has been catalogued with Document No. NAPS-01408 with the ASIS National Auxiliary Publication Service, c/o CCM Information Corp., 866 Third Ave., New York, N.Y., 10022. A copy may be obtained by citing the document number and by remitting \$1.00 for microfiche or \$3.00 for photocopies. Advance payment is required. Make checks or money orders payable to: CCMIC-NAPS.

¹² O. Aksnes and O. Foss, *Acta Chem. Scand.* **8**, 1787 (1954).

¹³ F. H. Kruse, R. E. Marsh, and J. D. McCullough, *Acta Crystallogr.* **10**, 201 (1957).

¹⁴ O. Foss, K. Johnsen, and T. Reistad, *Acta Chem. Scand.* **18**, 2345 (1964).

¹⁵ R. E. Marsh, *Acta Cryst.* **5**, 458 (1952).

¹⁶ H. T. Palmer and R. A. Palmer, *Acta Cryst.* **B25**, 1090 (1969).

¹⁷ D. Sutler, H. Dreizler, and H. D. Rudolph, *Z. Naturforsch.* **20a**, 1676 (1965).

Calculation of Collision-Broadened Linewidths in the Infrared Bands of Methane*

G. D. T. TEJWANI AND P. VARANASI

Department of Mechanics, State University of New York, Stony Brook, New York 11790

(Received 22 February 1971)

Anderson-Tsao-Curnutte theory of collision-broadened spectral lines has been extended to octopolar molecules, and the results are applied to the rotational lines in the ν_3 band of methane. Calculated half-widths are in excellent agreement with the high-resolution measurements of Varanasi for self-broadening and broadening by N_2 , O_2 , H_2 , and He. The theory has also been applied to CO lines broadened by CH_4 and to CH_4 lines broadened by HCl. The excellent agreement with experimental data in both the cases leads to the estimate of $\Omega = 5.0 \times 10^{-34}$ esu·cm³ for the octopole moment of CH_4 .

I. INTRODUCTION

Anderson's theory¹ of collision broadening of spectral lines, as expounded by Tsao and Curnutte,² has been most successfully applied to many cases. These include self-broadening and foreign gas broadening of linear, symmetric-top and asymmetric-top molecules. A critical review of the theory, its application to various cases of molecular interactions, and the references to the work of several authors are given by Birnbaum.³ However, a careful look at all the published literature indicates that the theory has not been extended to collisions involving molecules having only an octopole moment as their first nonvanishing permanent moment. A practically important application of such an extension of the theory presents itself in the case of the infrared lines of the methane molecule. A detailed knowledge of the collision-broadened half-widths of methane lines broadened by nitrogen, hydrogen, and helium are of enormous importance in calculating the abundance of this molecule in planetary atmospheres.

Due to the complex structure of the infrared spectrum of methane, it is not always possible to measure accurately the half-widths of methane lines. In fact, direct measurement^{4,5} of linewidth is possible only for lines with the rotational quantum number $J \leq 2$. Furthermore, it has been found experimentally⁴ that, while the optical collision diameters of methane lines broadened by foreign gases (especially H_2 , O_2 , and He) are very close to those derivable from transport properties according to the kinetic theory of gases, the diameters for self-broadening are very much larger. Thus, it appears highly desirable to attempt an extension and application of Anderson's theory to methane lines. An attempt has been made recently quite successfully by Tejwani⁶ and we present below the essential features of his work and a comparison with the measurements of Varanasi⁴ on the ν_3 fundamental.

One does not fail to notice in the critical article by Stogryn and Stogryn⁷ on molecular moments that there still exists a great deal of uncertainty as to the precise value of the octopole moment of CH_4 . They recommend